Comparison between the switching dynamics of homeotropic and planar cells of chiral smectic-*C* liquid crystals

N. Pereda,[1] J. Ortega,[2] C. L. Folcia,[1] and J. Etxebarria[1]
[1]*Departmento de Física de la Materia Condensada, Facultad de Ciencias, Universidad del País Vasco, Apartado 644, 48080 Bilbao, Spain*
[2]*Departamento de Física Aplicada II, Facultad de Ciencias, Universidad del País Vasco, Apartado 644, 48080 Bilbao, Spain*
(Received 22 February 2000)

The molecular dynamics during the switching of homeotropic and planar cells of chiral smectic-*C* liquid crystals has been investigated using electrooptic measurements and second-harmonic-generation interferometry. Two ferroelectric liquid crystals with great differences in their molecular structures have been studied. It has been found that the molecular motion is rather different depending on the type of cell used. For planar cells, the azimuthal rotation of the molecules is limited within half the smectic cone and the molecules rotate in opposite directions in the two halves of the chevron structure. In contrast, for homeotropic cells there is no chevron structure and a uniform macroscopic optical indicatrix can be defined all over the sample during the whole switching process. However, the molecular reorientation takes place within numerous microdomains of size smaller than the optical wavelength. There are two types of microdomains that occur with different probabilities depending on the material. Within each domain the molecules rotate in opposite directions, and the molecules describe a complete cone during a whole switching period.

PACS number(s): 61.30.−v, 78.20.Jq, 42.65.Ky

I. INTRODUCTION

In a previous paper [1], the switching dynamics of homeotropically aligned chiral smectic-*C* (Sm*C**) materials under a bipolar square-wave electric field was investigated. It was concluded that the molecular reorientation goes on within numerous microdomains of size smaller than the optical wavelength. Two types of microdomains can be found with different probabilities, and in each of them the director rotates in opposite directions, describing a complete cone during the whole switching period. These results are not in complete agreement with other studies carried out before [2].

The situation is schematized in Fig. 1. Upon field reversal from $+\mathbf{E}$ to $-\mathbf{E}$, there is a proportion x of molecules (with director $\mathbf{n}_+$) switching on the upper side of the tilt cone. At the same time, a proportion $(1-x)$ of molecules (with director $\mathbf{n}_-$) switches along the lower side of the cone. Furthermore, when the field changes from $-\mathbf{E}$ to $+\mathbf{E}$, the direction of the rotation of $\mathbf{n}_+$ (or $\mathbf{n}_-$) is not reversed, but the azimuthal angle φ (or $-\varphi$) continues to increase monotonically from 180° to 360°.

These results are rather surprising, because it can be shown that, unless $x=\frac{1}{2}$, this switching mechanism is not compatible with the twofold symmetry of the Sm*C** along the direction of the spontaneous polarization $\mathbf{P}_s$. In Ref. [1], these conclusions were established for usual calamitic materials and, thus we have considered it of interest to check further the generality of this behavior in other types of Sm*C** structures. With this aim, in this work we have investigated, at different temperatures, the switching characteristics of two ferroelectric liquid crystals (FLC's) that present great differences in their molecular structure. The study was carried out by means of electro-optic (EO) and second-harmonic-generation (SHG) interferometry measurements. The application of these techniques was also extended to the investigation of the switching dynamics in planar cells, where the sample surfaces have a great influence, and the problem has been more extensively discussed [3–11]. We have compared both types of mechanisms, and analyzed their similarities and differences.

II. MATERIALS AND EXPERIMENTAL DEVICES

Two FLC compounds with different molecular structure were chosen for our investigations. One of them is the previously studied W316 [1], which is calamitic and presents a phase sequence Sm*C**-60 °C-Sm*A*-90 °C-Iso [12] and a high spontaneous polarization in the ferroelectric phase ($P_s = 360\,\mathrm{nC/cm^2}$ at room temperature [13]). The second one is an *ortho*-platinated β-diketonate complex (Pt1) of the family of (noncalamitic) compounds studied in Ref. [14]. Its phase sequence is Cry*-70 °C-Sm*C**-95 °C-Sm*A*-105 °C-Iso and

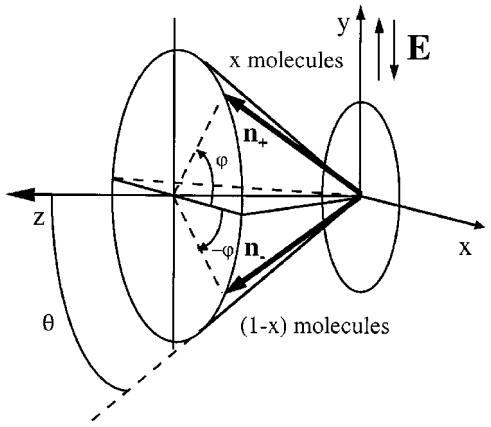

FIG. 1. Molecular motion during the switching of homeotropic cells of a Sm*C** liquid crystal. Two kinds of microdomains characterized by the directors $\mathbf{n}_+$ and $\mathbf{n}_-$ can be found in the sample, with probabilities x and $(1-x)$, respectively. Within each domain, $\mathbf{n}_+$ and $\mathbf{n}_-$ describe a complete cone in a whole switching period. The rotation is in opposite directions in the two types of domains.

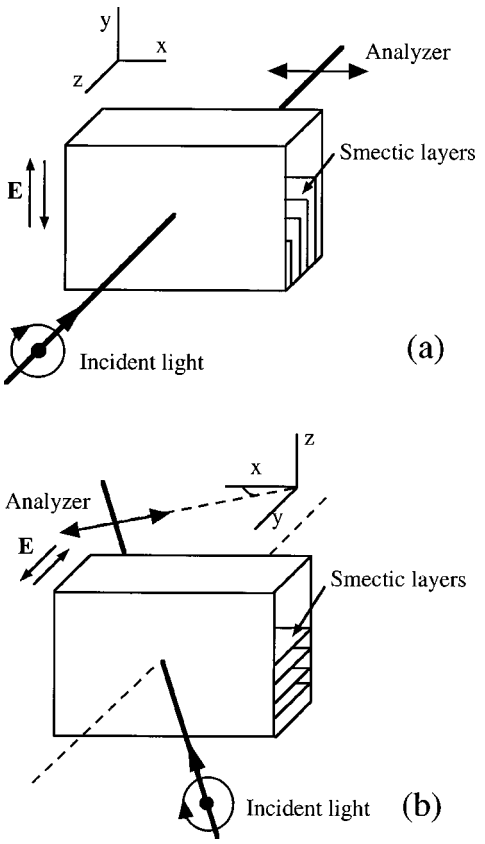

FIG. 2. Schematic diagram of the experimental setup for EO measurements in (a) homeotropic and (b) planar cells. The incident light is circularly polarized and the transmitted intensity is detected after passing the sample and a horizontal analyzer. The electric field is applied along the *y* axis. The coordinate systems correspond to that of Fig. 1.

it is characterized by a smaller P_s than W316 in the whole SmC^* temperature range ($P_s \sim 40\,\mathrm{nC/cm^2}$) [15].

Both planar and homeotropic samples were used in the present study. The materials were homeotropically aligned in glass cells treated with HTAB. The cell gap was maintained with two aluminum spacers of a nominal thickness of 10 μm which were also used as electrodes. On the other hand, commercial cells (EHC) of a nominal thickness of 4 μm were used for the planar samples. In both cases the cell thickness was determined accurately by means of an interferometric technique. The liquid crystalline materials were introduced into the cell in the isotropic phase. The cell was placed into a temperature-controlled stage with optical access. Good alignment was obtained in the SmC^* phase by slow cooling.

The EO measurements were carried out using an experimental setup that can be briefly described as follows. The light beam of a stabilized He-Ne laser (wavelength $\lambda = 632.8\,\mathrm{nm}$) was detected by a photodiode after passing a vertical polarizer, a $\lambda/4$ retarder set at 45° with respect to the vertical axis, the sample, and a horizontal analyzer. The homeotropic cells were fixed at normal incidence [see Fig. 2(a)], and a square-wave electric field of 1000 V/mm was applied along the vertical axis [*y* axis in Fig. 2(a)]. For studying the planar cells [see Fig. 2(b)], the sample was set at a non-null incidence, and it was arranged in such a way that the smectic layers were horizontally oriented [parallel to the *xy* plane in Fig. 2(b)]. An applied square-wave electric field

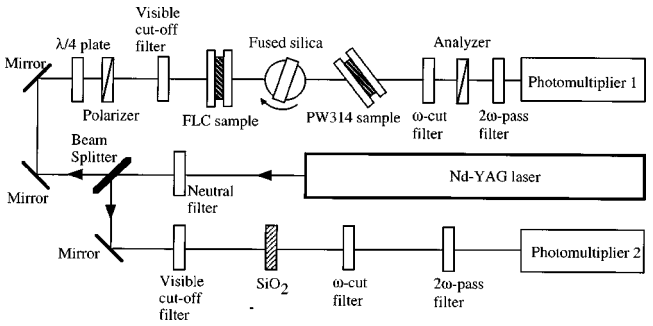

FIG. 3. Experimental setup for SHG interferometry. SHG waves are produced by the liquid-crystal sample and by a planar cell of a side-chain polymer (PW314). The relative phase between these two waves can be varied by rotating a fused silica plate placed in between. In addition, the phase between the applied electric field and the trigger of the laser can be changed, permitting then to measure the SHG signal generated by the liquid-crystal sample at different times during the switching.

of magnitude 2000 V/mm perpendicular to the glass plates was applied. In all cases the frequency of the field (about 5 Hz) was small enough to guarantee that equilibrium was attained before each field reversal. A real time detection of the signal was performed by means of a digital oscilloscope connected to the photodiode and triggered by the electric field generator.

Figure 3 shows the setup used for the SHG interferometry [16]. The fundamental light came from a *Q*-switched Nd:YAG laser (wavelength $\lambda = 1064\,\mathrm{nm}$, pulse width 6 ns, pulse frequency 5 Hz). The setup is quite similar to the one used in usual SHG experiments [17], except for some fundamental differences. In this case, a planar sample of a side-chain FLC homopolymer PW314 (whose SHG properties have been already studied [18]) was inserted at a certain incidence in the optical path. This particular sample was selected because it is quite stable at room temperature and produces SHG waves of the same order of magnitude as those generated by the studied FLC samples. A fused silica plate vertically set on a rotating stage was also placed between the homopolymer and the sample. Under these conditions, a relative phase change between the SHG fields generated by the sample and the homopolymer is produced as a consequence of the frequency dispersion of the refractive index of the silica plate. Therefore, interference fringes can be obtained when the silica plate is rotated and the optical path is consequently changed. The electric field applied to the FLC samples was in all cases the same as in the EO measurements. It was synchronized with the laser pulse and their relative phase could be suitably shifted. This permitted us to measure the SHG signal at any selected position of the molecules during their reorientation process. A reference branch, which measured the SHG light generated by a SiO_2 crystal, was used in order to compensate for the intensity fluctuations and laser pulse spreading with time.

III. EO MEASUREMENTS IN HOMEOTROPIC SAMPLES

Under the assumption of the switching model of Fig. 1, and taking into account that the domains with directors $\mathbf{n}_+$ and $\mathbf{n}_-$ are microscopic, the transmitted intensity I in the

geometry of Fig. 2(a) can be computed by first calculating the average optical dielectric tensor of the material, $\varepsilon = x\varepsilon_+ + (1-x)\varepsilon_-$, as a function of φ. Here $\varepsilon_+(\varepsilon_-)$ denotes the optical dielectric tensor corresponding to the $\mathbf{n}_+$ ($\mathbf{n}_-$) director in Fig. 1. A cumbersome but straightforward calculation leads us to the Jones matrix of the system, and the transmitted intensity results:

$$I \propto 1 + \sin 2\alpha \sin\left(\frac{2\pi \Delta n d}{\lambda}\right), \tag{1}$$

α being the angle that the optical indicatrix projected on the xy plane makes with the analyzer axis, Δn the birefringence at normal incidence, and d the sample thickness. Both α and Δn depend on the azimuthal angle φ of the director on the tilt cone, the relative microdomain populations x, and the tilt angle θ. It can be shown that $\Delta n = n_2 - n_1$ and α are given by

$$n_1^2 = n_o^2 + \frac{n_e^2 - n_o^2}{2}\Big[1 - \sqrt{x^2 + (1-x)^2 + 2x(1-x)\cos 4\varphi}\Big]\sin^2\theta, \tag{2}$$

$$n_2^2 = n_o^2 + \frac{n_e^2 - n_o^2}{2}\Big[1 + \sqrt{x^2 + (1-x)^2 + 2x(1-x)\cos 4\varphi}\Big]\sin^2\theta, \tag{3}$$

$$\tan\alpha = \frac{(2x-1)\sin 2\varphi}{\cos 2\varphi + \sqrt{x^2 + (1-x)^2 + 2x(1-x)\cos 4\varphi}}, \tag{4}$$

where n_e and n_o are the extraordinary and ordinary refractive indices of the material.

For $x = \frac{1}{2}$, which is the only possibility compatible with the SmC^* C_2 symmetry, Eq. (4) gives $\tan\alpha = 0$. Therefore, in this case I should be time-independent.

Figure 4 shows the I data for both materials at two representative temperatures within the SmC^* phases. Evidently, $x \neq \frac{1}{2}$ in either case. Furthermore, it can be seen that the signal behavior is the same independent of the switching direction. This characteristic can only be understood if α increases monotonically with time during the switching, irrespective of the particular switching model considered [see Eq. (1)]. In other words, the optical indicatrix must rotate in a definite direction and, therefore, the molecules must describe a complete cone. It must be noted that if the movement back and forth along half a cone had taken place, the second signal in Figs. 4(a) and 4(b) would have appeared inverted with respect to the first one. Similar measurements carried out at different temperatures within the SmC^* range in both materials revealed essentially the same behavior.

The continuous lines in Fig. 4 are the theoretical predictions assuming the simplest dynamic equation for the azimuthal angle,

$$\gamma \frac{d\varphi(t)}{dt} = P_s E \sin\varphi(t), \tag{5}$$

where γ is the rotational viscosity of the material. The agreement is satisfactory, although in the second part of the switching process a slowing down of the actual molecular motion, not explainable by Eq. (5), seems to occur.

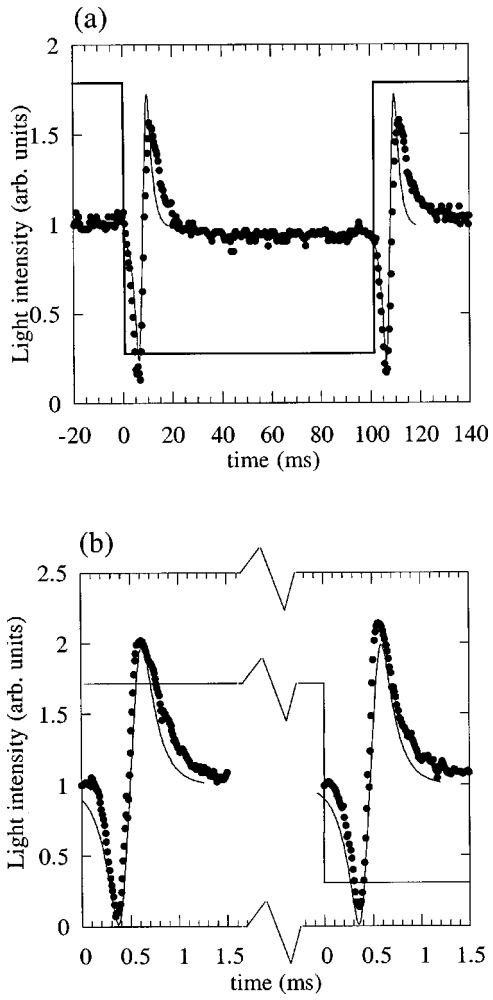

FIG. 4. Transmitted intensity versus time during the switching of a homeotropic cell of (a) Pt1 and (b) W316. The applied field frequency was 5 Hz in both cases. The signal behavior does not depend on the switching direction. The continuous lines are the best fits to the theoretical predictions. The data were taken at 80 and 45 °C, respectively.

The x and γ parameters that correspond to the best fits in Fig. 4 are presented in Table I. θ and Δn were measured independently, and P_s data were taken from the literature [13,15]. As can be seen, x shows no appreciable temperature variations within the experimental error in the range studied, whereas γ displays a typical Arrhenius behavior. The activation energies resulted to be $E_A = 19.2$ and 17.5 kcal/mol for Pt1 and W316, respectively.

IV. EO MEASUREMENTS IN PLANAR CELLS

The dynamic behavior in SmC^* planar samples has been thoroughly studied in the past and the switching mechanisms are quite well known [3–11]. However, several characteristics of the process are rather different from those we have found here for homeotropic samples. Therefore, it is interesting to analyze the phenomenon in planar cells and compare the results using similar experimental procedures. This comparative study was only performed on W316.

The molecular motion during the switching in planar cells

TABLE I. Relative microdomain populations x and rotational viscosity γ of the studied materials at various temperatures in the SmC^* phase. T_c: SmA-SmC^* transition temperature. θ and Δn were measured on a polarizing microscope using an EO method and a Berek compensator, respectively. P_s data were taken from Ref. [15].

Compound	$T_c - T$ (°C)	θ (deg)	Δn	P_s (nC/cm^2)	x	γ (Pa s)
W316	31	24	0.135	360	0.9	3.6
	28.5	23.8	0.135	360	0.9	2.57
	26	23.5	0.135	360	0.9	1.71
	21	23	0.135	340	0.9	1.0
	16	21.2	0.135	320	0.9	0.69
	11	18.5	0.135	290	0.9	0.47
	6	15.3	0.135	250	0.9	0.27
Pt1	15	18.2	0.121	42	0.73	0.93
	10	16	0.116	37	0.74	0.46
	5	10	0.112	27	0.74	0.22

is schematized in Fig. 5. According to the most widely extended model, the azimuthal rotation of the liquid-crystal molecules is limited within half the cone, and the molecules undergo counterazimuthal rotation in the upper and lower halves of the chevron structure [4,9,11].

Figure 6 shows the light transmission data in the disposition of Fig. 2(b) for both reversals of the electric field. The data refer to a sample of 4.9 μm at 25 °C. The angle of incidence was 45°. As is observed, the transmitted signal becomes inverted when the electric field is inverted. This result can be explained only if the dipole moments of the molecules rotate from 0° to 180° back and forth in both halves of the chevron (see Fig. 5). A rotation from 0° to 360° would have given rise (except in the case of normal incidence) to different signal profiles for both reversals of the field.

The data of Fig. 6 can also be interpreted quantitatively. Unfortunately, in this case there is not a simple analytical expression that accounts for the observed signal. This is mainly due to the inhomogeneity of the sample because of the existence of two (macroscopically different) chevron halves. Thus, the only feasible way to analyze the data is numerically. This has been done using a computer program that simulates different switching models, where the molecules may describe either a cone or half a cone, and the relative size of the chevron halves can be varied. Figure 7 shows the comparison between the experimental data and the theoretical predictions using the model of Fig. 5 with $\varphi(t)$

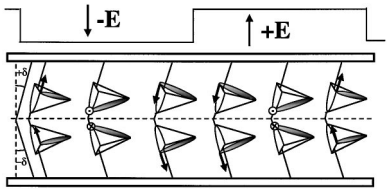

FIG. 5. Molecular motion during the field inversion in planar cells. The molecules rotate toward opposite directions in the upper and lower halves of the chevron, describing half a cone.

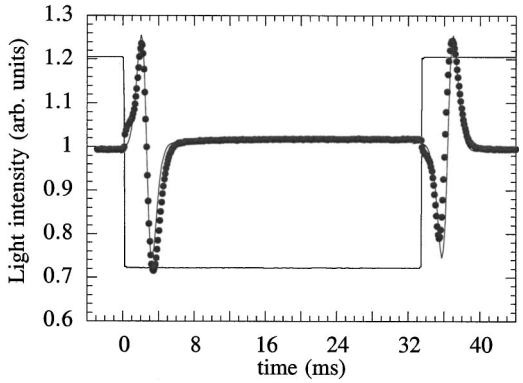

FIG. 6. Dependence of the transmitted intensity on time during the switching of a planar cell of W316. The signal becomes inverted when the switching direction is reversed.

given by Eq. (5). The best agreement is obtained for slightly different sizes of the two domains (asymmetric chevron), which seems reasonable and can be explained in terms of an asymmetric influence from both surfaces. Again, the last part of the curve is not perfectly reproduced as in the case of homeotropic samples.

V. SHG INTERFEROMETRY

The SHG interference experiments were carried out with the purpose of confirming the interpretation deduced from the previous EO studies. In this section we will analyze again the important question of the $\varphi(t)$ range described by the molecules during the switching.

Both homeotropic and planar samples were set at normal incidence, and the planar cells were disposed with the smectic layers horizontally oriented (Fig. 8). For homeotropic cells the relative phase between the applied electric field and the laser trigger was selected in such a way that maximum SHG intensity was detected when the polarizer and analyzer were vertical and horizontal, respectively. In this situation it can be shown that the azimuthal molecular angle is $\varphi = 90°$ (or $-90°$) and the fields configuration corresponds to the normal ee-o conversion (see Ref. [1]). In the case of planar cells, the azimuth $\varphi = \pm 90°$ was tuned from the fact that no

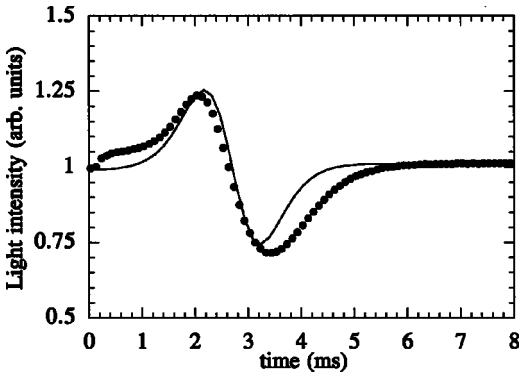

FIG. 7. Comparison between the experimental data of a planar cell of 4.9 μm of W316 (circles) and theoretical predictions (continuous line) according to the switching model of Fig. 5. The best agreement corresponds to a slightly different thickness for the two chevron halves (2.55 and 2.35 μm).

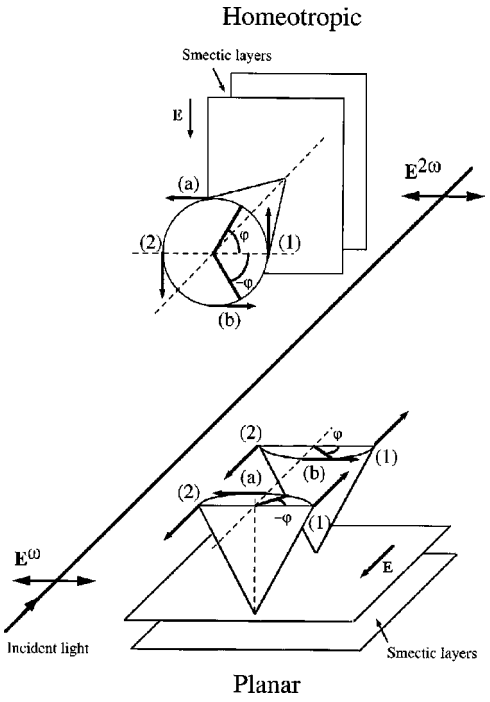

FIG. 8. Schematic representation of the experimental geometry used for the SHG interference measurements. The system is assumed to switch from (1) to (2). SHG signals were measured as a function of the incidence angle of the silica plate (Fig. 3) when the azimuthal molecular angles were $\varphi = \pm 90°$ [positions (a) and (b)].

vertically polarized SHG signal was generated by the sample upon illumination with vertically polarized incident light (null *ee-e* conversion). For the SHG interference experiments the incident light was polarized in the horizontal plane and the SHG wave was detected after passing a horizontal analyzer (*oo-o* conversion, see Fig. 8).

It can be shown that the SHG field $E_1^{(2\omega)}$ generated by the sample is horizontally oriented both for homeotropic and planar geometry [19]. Furthermore, the directional sense of the SHG field is reversed depending on the side of the cone chosen by the molecules during the switching ($+E_1^{(2\omega)}$ or $-E_1^{(2\omega)}$). If we denote $E_2^{(2\omega)}$ to the horizontal component of the SHG field generated by the polymer material, then the SHG intensity $I^{(2\omega)}$ detected by the photomultiplier (Fig. 3) is given by

$$I^{(2\omega)} \propto \left| E_1^{(2\omega)} + E_2^{(2\omega)} \exp\left[i\left(\frac{4\pi d_s \Delta n_d}{\lambda \cos \theta_r} \right) \right] \right|^2 . \qquad (6)$$

Here, d_s is the thickness of the silica plate, $\Delta n_d = n^{(2\omega)} - n^{(\omega)}$ accounts for the refractive index dispersion, and θ_r is the angle of refraction. Under these conditions, interference fringes are obtained if the fused silica plate is rotated around its vertical axis, thus varying θ_r.

Measurements as a function of the angle of incidence of the fused silica plate were carried out for both signs of the square-wave electric field (the same experiment was repeated after increasing in 180° the phase shift between the field and the laser trigger). Figure 9 shows the results for homeotropic samples of Pt1 and W316, and in Fig. 10 we have plotted the SHG interferograms for the case of a planar sample of W316. The obtained interference patterns are out of phase in

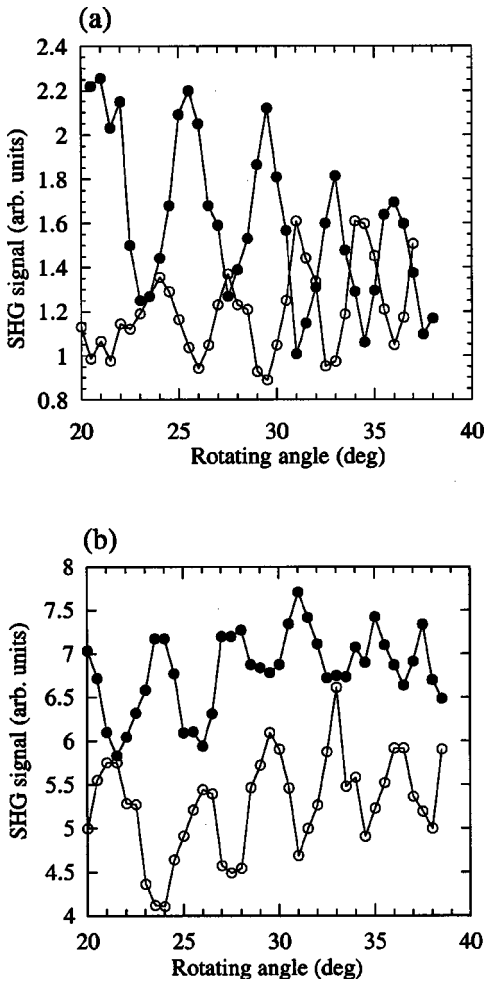

FIG. 9. Interference fringes of the SHG signals for (a) Pt1 and (b) W316 homeotropic samples. The data were taken at $T = 80$ and 25 °C, respectively. Closed and open circles correspond to opposite electric fields on the samples, with a time difference between them of half a switching period.

the case of the homeotropic geometry, which indicates that the FLC molecules have changed from $\varphi = 90°$ to $-90°$ (or vice versa) during the field inversion. On the other hand, in-phase signals are observed in the planar case, which evidences that no variation of the azimuthal angles has taken place during the process [20]. We are therefore led to the

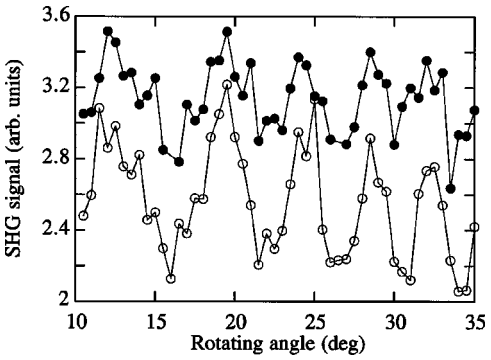

FIG. 10. SHG interferograms for a planar sample of W316 at 25 °C. Closed and open circles correspond to opposite electric fields on the sample, with a relative phase shift of 180°.

same conclusion as before, namely that during the whole switching period FLC molecules in homeotropic cells rotate from 0° to 360° whereas a back and forth rotation limited to half a cone occurs for planar cells.

VI. CONCLUSIONS

The switching characteristics under a square-wave electric field have been studied in homeotropic and planar FLC cells by means of EO and SHG interference measurements. These are independent and self-contained techniques, and have led us to obtain equivalent results. The present study was performed on FLC's with very different molecular structures, which, together with previously reported results, give us some confidence in the generality of the conclusions that can be drawn.

It is clear that at least two alternative switching mechanisms occur in FLC samples depending on the type of alignment. The different switching dynamics is a consequence of the boundary conditions to which the system is subjected in each case.

For planar cells the surface interactions compel the molecules to choose one particular half of the smectic cone during the switching. On the other hand, although for homeotropic cells it would seem reasonable to think that the molecules are free of surface constraints, the observations reported in the present study are not in agreement with this idea. The existence of a privileged type of microdomains ($x \neq \frac{1}{2}$), where the molecules rotate from 0° to 360°, implies a breakdown of the twofold symmetry of the cell (a C_2 axis along the **E** field direction would prohibit the macroscopic optical indicatrix to rotate in a particular direction). Probably the symmetry reduction should occur via a tilt of the smectic layers as has been pointed out in Ref. [1]. Anyway, it is the cell surfaces which are, in the last instance, responsible for this symmetry reduction. In this respect, it would be interesting to test homeotropic cells with different alignment agents or even to perform measurements on freely suspended films in order to examine other kinds of surface conditions.

ACKNOWLEDGMENTS

One of us (N.P.) is grateful to the Ministry of Education of Spain for a grant. This work was supported by the CICYT of Spain (Project No. MAT97-0986-02) and by the Universidad del País Vasco (Project No. 063.310-EB158/97).

[1] N. Pereda, C. L. Folcia, J. Etxebarria, and J. Ortega, Phys. Rev. E **61**, 2799 (2000).
[2] I. Drevensek Olenik, R. Torre, and M. Copic, Phys. Rev. E **50**, 3766 (1994).
[3] X. Jiu-Zhi, M. A. Handschy, and N. A. Clark, Ferroelectrics **73**, 305 (1987).
[4] Y. Ouchi, H. Takano, H. Takezoe, and A. Fukuda, Jpn. J. Appl. Phys., Part 2 **26**, L21 (1987).
[5] Y. Ouchi, H. Takezoe, and A. Fukuda, Jpn. J. Appl. Phys., Part 1 **26**, 1 (1987).
[6] W. Hartmann, Ferroelectrics **85**, 455 (1988).
[7] L. A. Beresnev and L. M. Blinov, Ferroelectrics **92**, 729 (1989).
[8] J. W. Goodby, R. Blinc, N. A. Clark, S. T. Lagerwall, M. A. Osipov, S. A. Pikin, T. Sakurai, K. Yoshino, and B. Zeks, in *Ferroelectric Liquid Crystals: Principles, Properties and Applications*, Vol. 7 of *Ferroelectricity and Related Phenomena*, edited by G. W. Taylor (Gordon and Breach, Philadelphia, 1991).
[9] B. Park, M. Nakata, S. S. Seomun, Y. Takanishi, K. Ishikawa, and H. Takezoe, Phys. Rev. E **59**, R3815 (1999).
[10] B. Park, S. S. Seomun, M. Nakata, M. Takahashi, Y. Takanishi, K. Ishikawa, and H. Takezoe, Jpn. J. Appl. Phys., Part 1 **38**, 1474 (1999).
[11] D. S. Pabla, and S. J. Elston, Liq. Cryst. **27**, 183 (2000).
[12] D. M. Walba, M. B. Ros, N. A. Clark, R. Shao, K. M. Johnson, M. G. Robinson, J. Y. Liu, and D. J. Doroski, Mol. Cryst. Liq. Cryst. **198**, 51 (1991).
[13] D. Hermann, L. Komitov, S. T. Lagerwall, G. Anderson, R. Shashidar, J. V. Selinger, and F. Gießelmann, Ferroelectrics **181**, 371 (1996).
[14] J. Ortega, C. L. Folcia, J. Etxebarria, M. B. Ros, and J. A. Miguel, Liq. Cryst. **23**, 285 (1997).
[15] M. B. Ros (private communication).
[16] S.-W. Choi, Y. Kinoshita, B. Park, H. Takezoe, T. Niori, and J. Watanabe, Jpn. J. Appl. Phys., Part 1 **37**, 3408 (1998).
[17] N. Pereda, C. L. Folcia, J. Etxebarria, J. Ortega, and M. B. Ros, Liq. Cryst. **24**, 451 (1998).
[18] N. Pereda, J. Etxebarria, J. Ortega, C. L. Folcia, C. Artal, M. B. Ros, and J. L. Serrano (unpublished).
[19] In general, $E_1^{2\omega} \neq 0$. For homeotropic samples, the condition $E_1^{2\omega}=0$ is only attained if x is exactly $\frac{1}{2}$. For planar cells $E_1^{2\omega}$ may be null if the SHG waves from the two chevron halves cancel exactly in amplitude and phase. This would happen, e.g., for a symmetric chevron if, in addition, the ratio between the sample thickness and the SHG coherence length is four times an integer. None of our samples verified these peculiar conditions.
[20] A similar result in planar cells was obtained by Park *et al.* (Ref. [9]) for a smectic sample showing V-shaped switching.